Experimental Study on Flow Boiling Heat Transfer Characteristic in Top-Connected Microchannels with a Ni/Ag Micro/nano Composite Structure

Zeyu Xu , Wei Zhang * , Qianqian Zhang , Xiangrui Zhai , Xufei Yang * , Yajun Deng , Xi Wang

Posted Date: 18 February 2025

doi: 10.20944/preprints202502.1397.v1

Keywords: microchannel; flow boiling; heat transfer enhancement; Ni/Ag micro/nano composite structure; wettability

 doi:10.20944/preprints202502.1397.v1

Article

Experimental Study on Flow Boiling Heat Transfer Characteristic in Top- Connected Microchannels with a Ni/Ag Micro/nano Composite Structure

Zeyu Xu, Wei Zhang *, Qianqian Zhang, Xiangrui Zhai, Xufei Yang, Yajun Deng, Xi Wang and Bo Yu

Beijing Key Laboratory of Pipeline Critical Technology and Equipment for Deepwater Oil & Gas Development, School of Mechanical Engineering, Beijing Institute of Petrochemical Technology, Beijing 102617, China

* Correspondence: vzhang@bipt.edu.cn

Abstract: Microchannel heat exchangers have a large specific surface area, which endows them with high heat and mass transfer efficiency and broad application prospects in fields such as chemical engineering and energy. Aiming at enhancing the flow boiling heat transfer in microchannels, a top-connected microchannel heat exchanger with a Ni/Ag micro/nano composite structure surface was designed. This top-connected microchannel consists of 11 parallel microchannels. The cross - section of each microchannel is a square with a size of 400 μm×400 μm, and the height of the connected space above the parallel channels is also 400 μm. The Ni/Ag micro/nano composite structure was prepared on the surface of the top-connected microchannel by the brush - plating technique. Using anhydrous ethanol as the working fluid, a comparative experimental study on flow boiling heat transfer in regular parallel microchannels (Regular Microchannel - RMC), top-connected microchannels (Top-connected Microchannel-TCMC), and top-connected microchannels with a micro/nano composite structure surface (TCMC-Ni/Ag) was carried out. The results show that the maximum local heat transfer coefficient of the TCMC-Ni/Ag surface reaches 179.84 kW/m²·K, which is 4.1 times higher than that of the RMC. Visualization studies have found that for TCMC-Ni/Ag, the strongly hydrophilic micro/nano composite structure surface simultaneously increases the nucleation density and nucleation frequency. Under medium and low heat flux conditions, a flow pattern structure is formed where the gas phase converges in the top-connected region while a large number of bubbles still form on the microchannel surface. Under high heat flux density conditions, the capillary liquid absorption effect of the strongly hydrophilic micro/nano composite structure leads to a thin-liquid - film convective evaporation heat transfer mode in the channel, which is the main mechanism for the significant improvement of its heat transfer performance.

Keywords: microchannel; flow boiling; heat transfer enhancement; Ni/Ag micro/nano composite structure; wettability

1. Introduction

Microchannels, distinguished by their characteristic dimensions spanning the micron - to - sub - millimeter scale, exhibit a remarkable combination of a large specific surface area and low thermal inertia. This unique set of attributes endows microchannels with an inherently high efficiency in heat and mass transfer processes. The relatively large specific surface area provides an extensive interface for the exchange of heat and mass between the fluid flowing through the microchannels and the channel walls. Meanwhile, the low thermal inertia allows microchannels to respond rapidly to changes in heat input or fluid conditions, facilitating efficient energy transfer.

The concept of microchannel heat exchangers was initially introduced by Pease and Tuckerman [1]. Since then, an extensive body of research has been conducted by scholars both at home and abroad. This research has comprehensively explored various aspects within the microchannel

 doi:10.20944/preprints202502.1397.v1

context, including single - phase and phase change heat transfer mechanisms [2], heat transfer enhancement techniques [3], and the development of microchannel heat exchange equipment [4]. Specifically, the research on single - phase convective heat transfer in microchannels has predominantly focused on achieving a delicate balance. On one hand, there is a strong emphasis on augmenting the heat transfer coefficient to enhance the overall heat transfer rate. This is crucial as it directly impacts the efficiency of heat dissipation or utilization in microchannel - based systems. On the other hand, it is essential to mitigate the resistance penalty that often accompanies heat transfer enhancement measures. An increase in the heat transfer coefficient typically comes at the cost of an increased pressure drop, which requires additional pump power to maintain the fluid flow. This not only raises energy consumption but may also introduce limitations in terms of system design and operation. To achieve this balance, researchers have explored a variety of strategies. One approach involves optimizing the geometric configuration of the microchannels. This includes investigating different cross-sectional shapes, such as circular, rectangular, triangular, and trapezoidal. Each shape exhibits distinct hydrodynamic and heat transfer characteristics. For example, rectangular microchannels are often favored due to their relatively straightforward fabrication process and the ability to provide a larger surface area for heat transfer compared to circular channels of the same hydraulic diameter. By carefully adjusting the aspect ratio (the ratio of the channel width to height) of rectangular microchannels, it is possible to enhance heat transfer while keeping the pressure drop within an acceptable range.

Another strategy is engineering surface microstructures on the inner walls of the microchannels. These microstructures can take various forms, from simple protrusions and indentations to more complex patterns like microfins, microgrooves, and micropillars. The presence of these surface features disrupts the laminar flow near the wall, promoting fluid mixing and enhancing heat transfer. Microfins, for instance, can increase the heat transfer coefficient by creating additional turbulence and extending the heat transfer area. However, these structures also increase the surface roughness, which in turn raises the frictional resistance. Therefore, meticulous design and optimization of these micro - structures are necessary to maximize the heat transfer enhancement while minimizing the resistance penalty.

Increasing the pump power is also considered as a means to enhance single phase convective heat transfer. By increasing the flow velocity of the fluid, the convective heat transfer coefficient can be increased due to the enhanced mixing and reduced thickness of the thermal boundary layer. Nevertheless, this approach is limited by the power consumption of the pump and the mechanical constraints of the system. High - velocity flows can lead to issues such as cavitation and erosion in the microchannels, which can damage the microchannel structure and compromise its long - term performance.

The fundamental principles underlying heat transfer enhancement in single - phase convective heat transfer in microchannels revolve around two key aspects. Firstly, intensifying fluid disturbance within the mainstream region of the microchannel can enhance the mixing of the fluid. This enhanced mixing improves the heat transfer rate as it allows for more efficient transfer of heat from the channel walls to the bulk fluid. This can be achieved through the geometric design of the channels and the engineering of surface microstructures, as previously mentioned. Secondly, modulating the thermal boundary layer in the near - wall region is of utmost importance. The thermal boundary layer is the region near the channel wall where the temperature of the fluid changes significantly. By disrupting this layer, heat can be transferred more efficiently from the wall to the bulk fluid. This can be accomplished by creating vortices or secondary flows near the wall, which can carry the heated fluid away from the wall and replace it with cooler fluid from the mainstream [5].

In contrast to single - phase convective heat transfer within microchannels, the phase change heat transfer process in microchannels is distinguished by a latent heat exchange that occurs during the gas - liquid phase transition. This phenomenon is pivotal, as it engenders a substantial increase in the heat transfer coefficient, which can rise by more than an order of magnitude compared to its single - phase counterpart. The significance of this enhancement cannot be overstated, as it endows

 doi:10.20944/preprints202502.1397.v1

high - efficiency cooling technologies founded on microchannel phase change heat transfer with great promise in diverse applications. Prominent among these are battery thermal management [6] and high - heat - flux chip cooling [7]. In battery thermal management, maintaining an optimal temperature is crucial for the performance, lifespan, and safety of batteries. Microchannel phase change heat transfer systems can effectively dissipate the heat generated during battery operation, ensuring stable performance. Similarly, in high - heat - flux chip cooling, where the escalating power density of modern chips demands advanced cooling solutions, the high - efficiency heat transfer capabilities of microchannel phase change mechanisms offer a viable approach to prevent overheating.

Notwithstanding these potential advantages, the practical realization of flow boiling heat transfer in microchannels is encumbered by several challenges. Foremost among these are flow instability [8] and critical heat flux density (CHF) [9].

Flow instability in microchannel flow boiling is a complex hydrodynamic issue that emerges from the intricate interactions between the liquid and vapor phases within the micro - scale confines. These interactions can disrupt the flow patterns, leading to pressure fluctuations and non - uniform distribution of the two - phase mixture, thereby deteriorating the heat transfer efficiency and potentially causing long - term damage to the microchannel heat exchanger.

The critical heat flux density represents another formidable challenge. As illustrated in Figure 1 [10], a plausible mechanism for CHF occurrence in microchannels is as follows: Once nucleated bubbles form within the microchannel, they rapidly expand due to the applied heat. Constrained by the narrow dimensions of the microchannel, these bubbles quickly fill the entire cross - section. With the channel walls restricting further cross - sectional expansion, the bubbles are compelled to grow longitudinally, forming an elongated, narrow extended - bubble flow. During this rapid expansion, the flow within the channel becomes unstable. In certain circumstances, the force exerted by the expanding bubbles can expel the upstream - flowing liquid from the channel, resulting in a local liquid deficiency in the downstream section. This deficiency, in turn, leads to a degradation of heat transfer efficiency, often accompanied by a significant increase in the microchannel surface temperature.

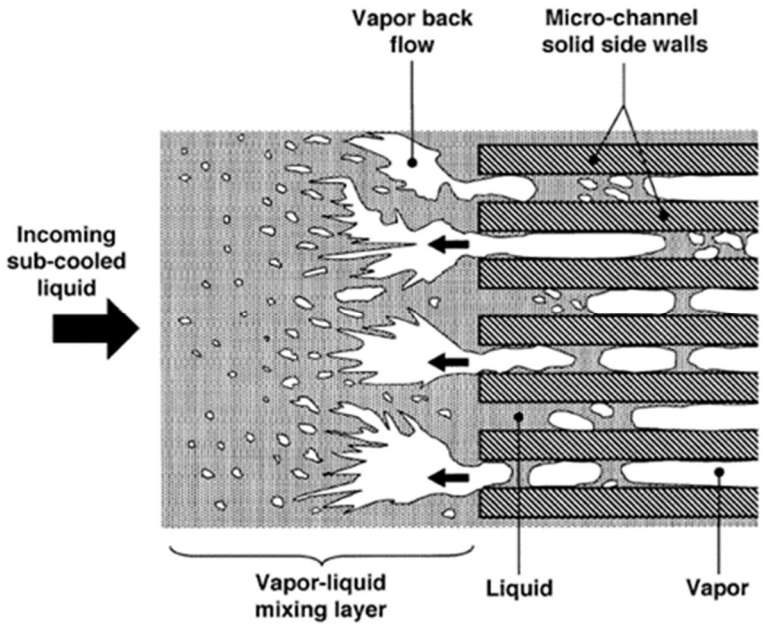

Figure 1. Schematic of vapor backflow as heat flux approaches CHF [10].

In the case of regular parallel microchannels, the situation is exacerbated. The rapid expansion of bubbles within the confined space along the channel direction can give rise to additional

 doi:10.20944/preprints202502.1397.v1

complications. Non - uniform flow distribution among the parallel channels is one such issue. Slight variations in local conditions, such as surface characteristics, heat flux distribution, and initial fluid properties, can cause differences in bubble growth and expansion rates. Channels with more conducive conditions for bubble formation may experience more rapid bubble expansion, which can impede liquid flow through these channels. This leads to an uneven distribution of the liquid - vapor mixture, with some channels receiving insufficient liquid for effective heat transfer, while others may be over - utilized, potentially creating local hotspots.

Furthermore, the non - uniform bubble expansion and flow distribution can generate local thermal stress among parallel channels. The differential heat transfer rates and fluid flow patterns induce temperature gradients between the channels. These temperature differences cause differential thermal expansion and contraction, which, over time, can lead to mechanical damage to the microchannel structure, such as crack formation or deformation. This not only compromises the long - term performance and reliability of the microchannel heat transfer system but also poses a significant obstacle to its practical implementation [11].

In the pursuit of enhancing heat transfer efficiency and suppressing flow instability within microchannel systems, Kalani and Kandlikar [12] put forward an innovative concept of a top-connected microchannel heat exchanger structure. This proposal stemmed from a comprehensive understanding of the complex hydrodynamics and heat transfer mechanisms in microchannels. They meticulously pointed out that this novel structure incorporates additional spaces specifically designed for vapor flow and pressure equilibrium located above the microchannels. These additional spaces play a pivotal role in the overall functionality of the system. By providing an extra pathway for vapor to escape and equilibrate the pressure, they can effectively mitigate the flow resistance that often plagues traditional microchannel designs. This reduction in flow resistance not only eases the passage of fluid through the microchannels but also serves to suppress the onset of flow instability, which is a common and detrimental issue in microchannel heat transfer processes.

Yin et al. [13,14] further delved into the practical implementation of this top-connected microchannel concept. They successfully fabricated a top-connected microchannel structure on the surface of a copper block, a material renowned for its excellent thermal conductivity. Through their experiments, they discovered an interesting phenomenon. Despite the fact that surface tension typically exerts a dominant influence inside the microchannels, a stratified gas - liquid flow pattern still emerged in the top-connected microchannels. This stratified flow pattern, distinct from the chaotic flow often associated with microchannel systems, was found to significantly improve the flow stability. This finding not only validated the theoretical advantages of the top-connected microchannel structure but also provided valuable insights into the complex fluid dynamics at play within these micro - scale systems.

Zhao et al. [15] focused their research on the flow boiling heat transfer characteristics within top-connected microchannels. Their in - depth study revealed that the heat transfer coefficient in these top-connected microchannels is significantly higher than that in ordinary parallel microchannels. This finding underscores the potential of the top-connected microchannel design in enhancing heat transfer performance. Moreover, their research identified three typical trends in the heat transfer coefficient as it varies with the change of vapor quality. These trends were closely associated with three distinct heat transfer modes: nucleate boiling, two - phase forced convection, and film boiling. They further determined that these heat transfer modes are dominated by the dimensionless boiling number, a crucial parameter that encapsulates the complex interplay between heat flux, mass flux, and fluid properties.

Notwithstanding the significant progress made in the research of top-connected microchannel heat exchangers, enhancing their phase change heat transfer performance remains a formidable and critical challenge. As the demand for more efficient heat transfer solutions continues to grow in various industries, such as electronics, energy, and automotive, further research is essential. This includes exploring novel materials, optimizing the geometric parameters of the microchannels, and

 doi:10.20944/preprints202502.1397.v1

developing advanced control strategies to better manage the complex phase change processes occurring within these micro - scale systems.

2. Concept

In the pursuit of augmenting the phase change heat transfer performance of top-connected microchannel heat exchangers, this paper introduces an innovative concept of a top-connected microchannel heat transfer structure integrated with a micro/nano composite surface structure. The underlying principle of this novel structure is elucidated in Figure 2. As depicted in Figure 2, the top-connected microchannels (TCMC, shown in Figure 2b) are constructed by creating a transverse connection region between the top cover plate and the microchannels of regular parallel microchannels (RMC, as presented in Figure 2a). This design feature enables the interconnection of different microchannels at their upper ends. During the bubble growth process within the microchannels, this interconnection allows the gas - liquid interface to expand both along and perpendicular to the flow direction. Consequently, issues such as pressure imbalance and flow rate pulsation, which typically arise in regular channels due to the non - synchronous nucleation and growth of bubbles, are effectively mitigated.

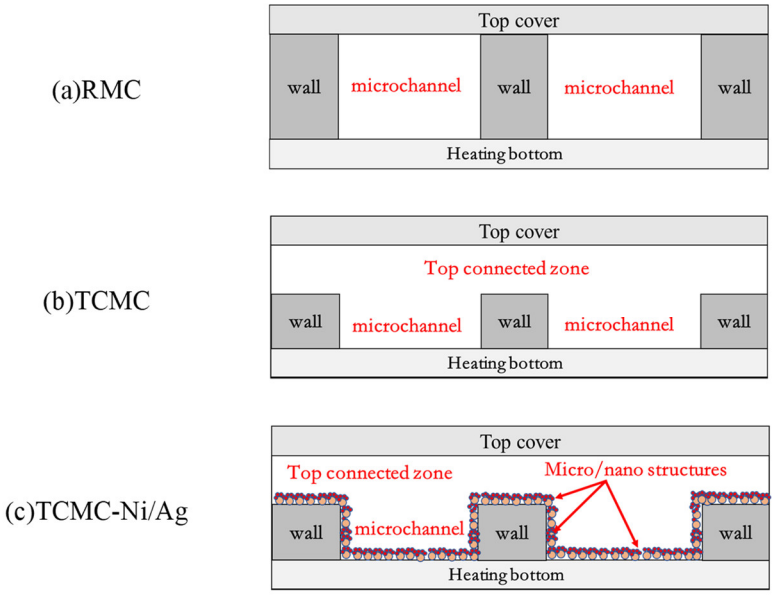

Figure 2. The main concept of the novel top connected microchannels covered with surface micro/nano composite structures. **(a)**the regular parallel microchannels; **(b)**the top-connected microchannels; **(c)** the novel top-connected microchannels with a micro/nano composite surface structure.

In this study, an additional innovation lies in the fabrication of a micro/nano composite structure on the entire surface of the microchannels in TCMC. This results in the formation of a top-connected microchannel with a multi - scale micro/nano composite surface (denoted as TCMC - Ni/Ag in Figure 2c). When compared to the regular parallel microchannels in Figure 2a and the improved top-connected open microchannels in Figure 2b, the novel TCMC - Ni/Ag structure brings about two significant changes. Firstly, it modifies the distribution of nucleation sites on the heating surface. Secondly, through the capillary driving effect generated by the multi - scale pores, it can regulate the hydrodynamic characteristics in the near - wall region. These combined effects lead to a substantial improvement in the phase change heat transfer performance.

The implications of this research are far-reaching. For the design and operation of high efficiency microchannel phase change heat exchangers, it provides crucial insights. By enhancing the heat

 doi:10.20944/preprints202502.1397.v1

transfer performance, it enables better heat dissipation, which is essential in various applications where heat management is critical. Moreover, improved heat transfer efficiency also contributes to more effective energy utilization, thereby promoting the development of sustainable and energy efficient technologies.

3. Experiments

This section may be divided by subheadings. It should provide a concise and precise description of the experimental results, their interpretation, as well as the experimental conclusions that can be drawn.

3.1. Fabrication of the test section

The experimental components were manufactured using copper as the base material. In the initial preparation stage, the copper substrate underwent surface treatment through polishing with 5000-grit sandpaper to achieve uniform smoothness. Subsequently, advanced laser etching technology was employed to create 11 parallel rectangular microchannels (RMC) with precise dimensional specifications: 18 mm in length, 0.4 mm in width, and 0.8 mm in depth. These microchannels were arranged with consistent 0.4 mm thick rib walls separating adjacent channels, ensuring structural regularity across the patterned surface.

For the top-connected microchannel configuration (TCMC), the fabrication process involved two-stage laser etching. Initially, a continuous shallow trench measuring 18 mm × 8.4 mm × 0.4 mm (length × width × depth) was etched across the polished copper surface to form an integrated top connection region. Following this primary etching phase, secondary processing was conducted to generate 11 parallel sub-channels within the base of the connected trench. These secondary microchannels maintained identical length (18 mm) and width (0.4 mm) parameters as the RMC configuration but with reduced height (0.4 mm), while preserving the 0.4 mm inter-channel spacing through precisely controlled laser parameters.

The Ni/Ag-TCMC variant was developed through surface modification using brush-plating technology [16,17], which involved three critical phases. The process commenced with electrochemical cleaning to ensure optimal surface activation, followed by deposition of an intermediate transition layer to enhance coating adhesion. The final stage implemented controlled current density plating to establish a hierarchical Ni/Ag micro-nano composite structure across the TCMC surface. This multi-step approach enabled the creation of a functionally graded surface architecture while maintaining the underlying microchannel geometry intact.

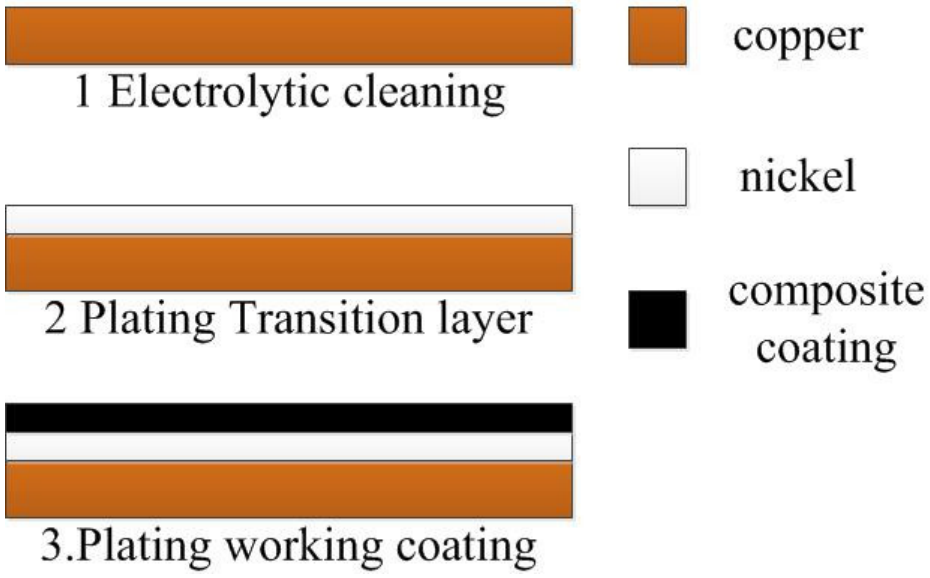

 doi:10.20944/preprints202502.1397.v1

Figure 3. The procedures of brush plating of Ni/Ag composite structures on copper.

As illustrated in Figure 4, the assembly drawing, physical diagram of the test section, and the cross-sectional view of the TCMC-type microchannel are comprehensively presented. To enable detailed visualization studies of the flow-pattern structures during flow boiling within the experimental section, the top cover plates of the microchannels are fabricated from high-purity, heat-resistant quartz glass. This material selection ensures both optical clarity for visualization and thermal stability under elevated operating conditions. The thermal energy required for the experiments is supplied by four precision electric heating cartridges, which are strategically embedded at the base of the copper block. These heating cartridges, with a diameter of 12 mm, a length of 64 mm, and a rated power of 220 W each, are designed to deliver uniform and controllable heat input to the test section. To optimize thermal management and minimize heat dissipation losses, the entire test section is encased in a polytetrafluoroethylene (PTFE) insulation layer. This PTFE casing not only reduces convective and radiative heat losses to the ambient environment but also ensures one-dimensional heat conduction along the vertical axis of the test section, thereby maintaining experimental consistency and accuracy.

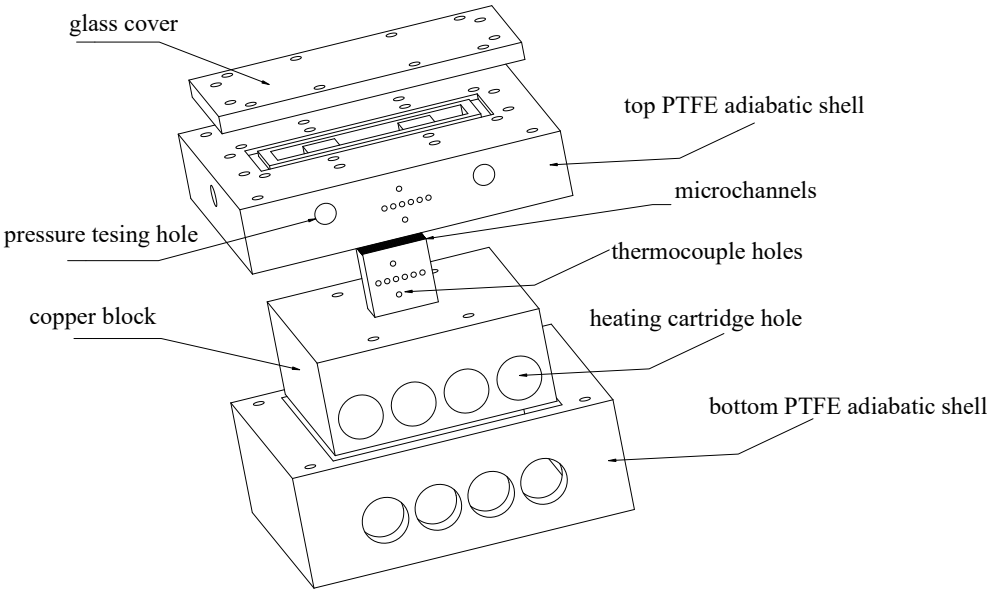

(**a**)

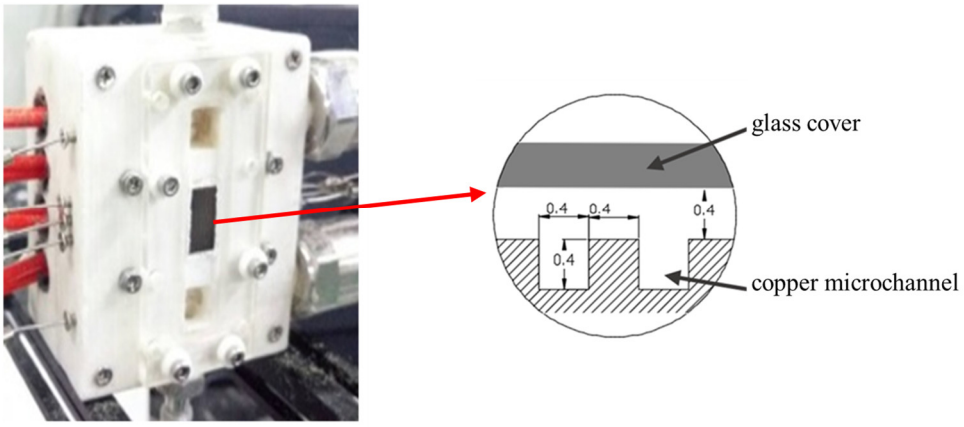

(**b**)

Figure 4. The test section and its assembly.

 doi:10.20944/preprints202502.1397.v1

Furthermore, the upper portion of the PTFE casing is equipped with eight temperature-measurement holes and two pressure-measurement holes, which are precisely aligned along the flow direction. High-precision K-type thermocouples, with a diameter of 1 mm and a temperature measurement accuracy of ±0.5 °C, are inserted into the temperature-measurement holes. These thermocouples facilitate the acquisition of real-time thermal data, enabling the calculation of heat flux and the characterization of temperature distribution along the flow path. The integration of these measurement systems ensures robust experimental control and reliable data collection for analyzing the thermal and hydrodynamic behavior within the microchannels.

3.2. The experimental setup

The experimental setup employed in this study is depicted in Figure 5. The working fluid housed within the liquid storage tank is expelled by a peristaltic pump. Subsequently, it traverses a flowmeter to quantify the flow rate, after which it is heated to a specific degree of sub - cooling by a pre - heater. The fluid then enters the experimental section, where heating induces a phase change heat transfer process. At the outlet of the experimental section, the generated steam is condensed by a condenser and subsequently returns to the liquid storage tank, thus completing a full cycle.

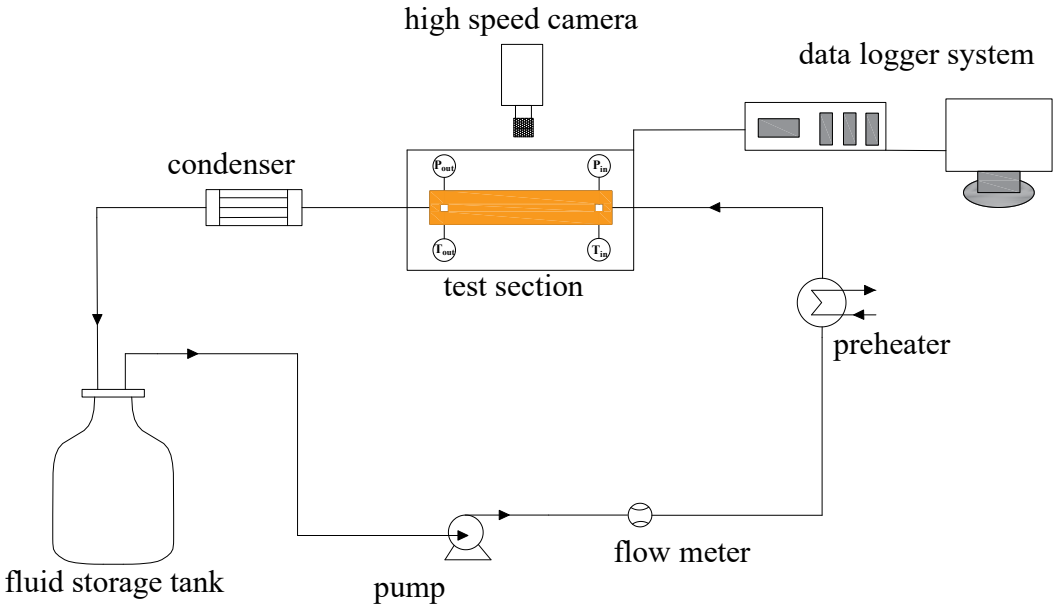

Figure 5. The experimental setup.

During the experimental procedure, the bubble dynamics and flow pattern transition characteristics within the micro - channels are captured by a high - speed camera positioned above the experimental section. The temperatures at the inlet and outlet of the experimental section, along with the temperature distribution along the flow path, are measured using a K - type thermocouple. The inlet and outlet pressures are determined by a pressure transmitter. The acquired data is collected via a data acquisition instrument and subsequently stored in a computer for subsequent postprocessing.

3.3. Data Processing and Uncertainty Analysis

As the working fluid at the inlet of the micro - channel is sub - cooled liquid, there exist a single - phase heat transfer region and a phase change heat transfer region after the working fluid enters the micro - channel. Therefore, the entire effective heating area can be divided into two regions along the flow direction, namely the single - phase convective heat transfer region and the two - phase phase change heat transfer region. Assuming that the heating quantity is uniformly distributed along

 doi:10.20944/preprints202502.1397.v1

the flow direction, the length of the single - phase flow region can be calculated through the energy conservation equation.

$$L_s = \frac{m(h_s - h_{in})L_h}{\eta Q} \quad (1)$$

where m is the mass flow rate, with the unit of kg/s ; L_h is the length of the micro - channel, with the unit of m; h_s is the enthalpy of the saturated working fluid, h_{in} is the enthalpy of the working fluid at the inlet, both with the unit of kJ/kg, Q is the heating power, with the unit of kW, and η is the thermal efficiency.

In the single - phase convection region, assuming that the temperature of the liquid is linearly distributed along the flow direction, the liquid temperature can be obtained through the following formula, with the unit of ℃.

$$T_{fx} = T_{in} + \frac{L_x(T_s - T_{in})}{L_s} \quad (2)$$

Here, T_{in} is the inlet temperature of the working fluid, and T_s is the saturation temperature of the working fluid, both measured in ℃. L_x denotes the length from the point where the temperature is to be determined to the inlet, while Ls represents the length of the single - phase convective heat - transfer zone, with the unit being m. In the two - phase flow region, the liquid temperature equals the saturation temperature of the working fluid. This saturation temperature is determined by using the average pressure at the inlet and outlet of the experimental section as the saturation pressure.

The local heat transfer coefficient along the experimental section h_x is calculated by Newton's law of cooling, with the unit of kW/m²·K.

$$h_x = \frac{q}{T_{wx} - T_{fx}} \quad (3)$$

Among them, q is the heat flux density with the unit of kW/m², T_{wx} is the wall temperature at this point, and T_{fx} is the liquid temperature corresponding to this point.

The uncertainty of experimental parameters consists of the uncertainty of directly - measured parameters and the uncertainty of indirectly - measured parameters. Directly - measured parameters include temperature and pressure directly measured by thermocouples and pressure sensors, which are mainly determined by the errors of the measuring sensors. That is, for a directly - measured parameter, we have Y_i:

$$Y_i = y_i + dy \quad (4)$$

where Y_i is the true value of the measured quantity; y_i is the actual measured value; and dy is the uncertainty of the measured quantity. For indirectly - measured parameters such as heat transfer coefficient and heat flux density, their uncertainties are calculated through the error transfer function of directly - measured parameters. Denote the indirectly - measured value as N，N=f(x_1，x_2，x_3，…，x_n)， where x_1，x_2，x_3，…，x_n are independent directly - measured values. Then the error of the indirectly - measured value can be calculated by the following transfer function:

$$S_N = \sqrt{\sum_1^n \left(\frac{\partial f(x_i)}{\partial x_i}\right)^2 (\delta x_i)^2} \quad (5)$$

Among them, S_N represents the standard error, and x_i denotes the relative error of the variable.

In the experiment, the maximum error of the K-type thermocouple used is approximately ±0.5 °C, the uncertainty of the heating power is ±2.0 W, and the machining dimensional accuracy is about ±0.02 mm. Through calculation, when the micro - channel surface reaches the critical heat flux density, the maximum relative error of the heat flux density is 2.6%, the maximum relative error of the wall temperature is 3.3%, and the maximum relative error of the heat transfer coefficient is 6.2%.

4. Results and Discussion

4.1. Characterization of Ni/Ag Micro/Nano Composite Structure

 doi:10.20944/preprints202502.1397.v1

Scanning electron microscopy (SEM, HITACHI, SU - 8010) was used to conduct a comparative analysis of the surface morphologies of the polished copper surface, the laser - etched surface, and the copper surface with the fabricated Ni/Ag micro/nano composite structure. The results are shown in Figure 6. It can be observed that on the polished copper surface, there are irregularly and sparsely distributed local cavities. The laser - etched surface has an ablated and uneven structure, with pores of various sizes on the ablated surface. The Ni/Ag micro/nano composite surface consists of densely arranged micro - sphere structures. The size of the micro - spheres is approximately 10~20 μm. There are papilla-like structures and cracks on the micro - spheres, and there are numerous pores of different scales between the microspheres.

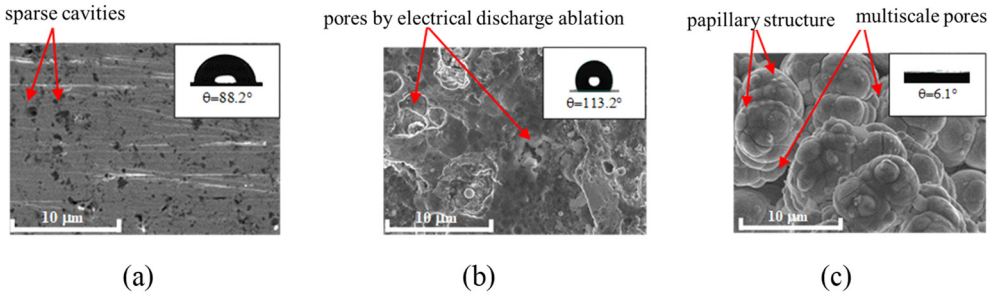

Figure 6. Surface structure morphology and contact angle. **(a)**plain copper surface;**(b)** surface formed by laser ablation;**(c)** surface covered with Ni/Ag composite structures.

An optical contact angle measuring instrument (Dataphysics OCA15 plus) was employed to measure the contact angles of 3.5 μL deionized water droplets on the smooth copper surface, the laser - etched surface, and the Ni/Ag micro/nano composite structure surface. The measured contact angles were 88.2°, 113.2°, and 6.1° (with an error of ±1.5°) respectively. That is, the laser - etched surface is hydrophobic, while the Ni/Ag micro/nano composite structure surface exhibits good hydrophilic properties.

4.2. Heat transfer characteristic

During the entire experimental process, the mass flow rate was kept constant at 0.95 g/s, and the heat flux density ranged from 326 kW/m² to 760 kW/m². Figure 7 shows the relationship between the heat transfer coefficient and the vapor quality of the three types of micro - channels under different working conditions. As can be seen from Figure 7a, in the ordinary parallel micro - channel (RMC), the heat transfer coefficient changes with the vapor quality in two trends: when the heat flux density is relatively small (q = 326 kW/m²), the heat transfer coefficient increases with the increase of the vapor quality; as the heating power increases (q = 543 kW/m² and 760 kW/m²), the heat transfer coefficient first increases and then decreases with the increase of the vapor quality. When q = 760 kW/m², the local maximum heat transfer coefficient reaches 35 kW/m²·K. Figure 7b shows the relationship between the heat transfer coefficient and the vapor quality in the top-connected microchannel (TCMC). For the working conditions with lower heating power (326 kW/m² and 543 kW/m²), the heat transfer coefficient increases monotonically with the increase of the vapor quality. For the high - heat - flux working condition (760 kW/m²), the change of the heat transfer coefficient with the vapor quality shows a three - stage trend, that is, the heat transfer coefficient first increases, then slightly decreases, and then continues to increase. And when q = 760 kW/m², the local maximum heat transfer coefficient reaches 44 kW/m²·K.

 doi:10.20944/preprints202502.1397.v1

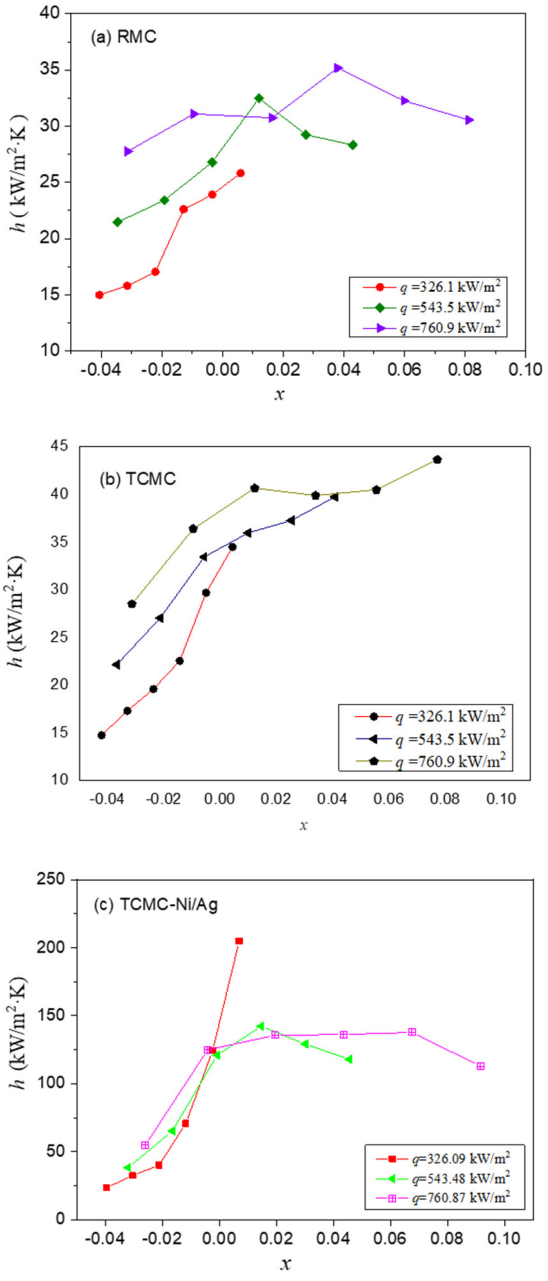

Figure 7. Variations of heat transfer coefficients with vapor quality.

Figure 7c shows the variation of the heat transfer coefficient with the vapor quality in the top-connected micro - channel with Ni/Ag composite micro/nano structure (TCMC - Ni/Ag). When the heat flux density is low (326 kW/m²), the heat transfer coefficient increases monotonically with the increase of the vapor quality; when the heat flux density is high, the heat transfer coefficient first increases and then remains basically unchanged with the increase of the vapor quality.

By comparing Figs. 7a, 7b and 7c, it can be found that for RMC, the heat transfer coefficient generally shows an increasing trend when the heat flux density increases; for TCMC, when the vapor quality is small, the heat flux density has a significant impact on the heat transfer coefficient, and as the vapor quality increases, the impact of the heat flux density on heat transfer weakens; for TCMC - Ni/Ag, in the low - vapor quality region where the vapor quality is less than zero, that is, corresponding to the subcooled boiling region, the heat flux density has a significant impact on the heat transfer coefficient, and as the vapor quality increases, the impact of the heat flux density on the heat transfer coefficient gradually weakens.

 doi:10.20944/preprints202502.1397.v1

The average heat transfer coefficients h_{avg} of three types of microchannels, namely RMC, TCMC, and TCMC - Ni/Ag, were calculated and compared, and the results are shown in Figure 8. Within the selected typical operating conditions, the average heat transfer coefficients of the three types of microchannels all increase with the increase of heat flux density. When q = 760 kW/m², the average heat transfer coefficients of RMC, TCMC, and TCMC - Ni/Ag reach their maximum values, which are 31.27 kW/m²·K, 38.28 kW/m²·K, and 116.98 kW/m²·K respectively. Under the same operating conditions, the average heat transfer coefficient of TCMC is increased by a maximum of 22% compared with that of RMC, while the average heat transfer coefficient of TCMC - Ni/Ag is increased by a maximum of 2.9 times compared with that of RMC

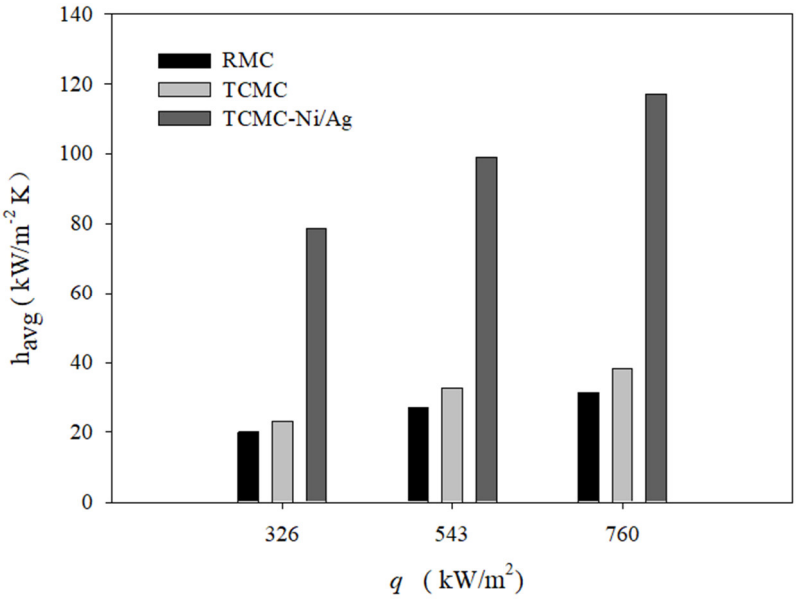

Figure 8. Comparison of averaged heat transfer coefficients.

4.3. Flow Pattern and Heat Transfer Enhancement Mechanisms

In order to profoundly disclose the mechanism underlying the enhanced flow boiling heat transfer within top-connected microchannels, a visualization study of the flow patterns in these microchannels was carried out using a CMOS camera (XIMEA, XIQ, Germany). Figure 9a presents an image of the typical flow - pattern structure within the TCMC. In the upstream microchannels and on the rib walls, relatively large nucleated bubbles are present, while in the downstream channels, elongated and narrow bubbles exist. Through observation, it was found that both isolated, elongated and narrow bubbles and coalesced large bubbles co - exist between adjacent channels. However, the coalescence of bubbles is more prone to occur along the flow direction, thereby forming an elongated and narrow bubble flow (or long slug) within the channel. In contrast, the phenomenon of bubble coalescence between adjacent channels in the direction perpendicular to the flow is relatively infrequent.

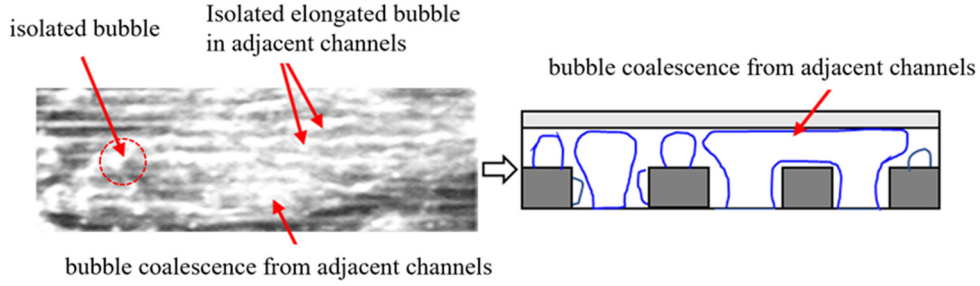

(**a**)

 doi:10.20944/preprints202502.1397.v1

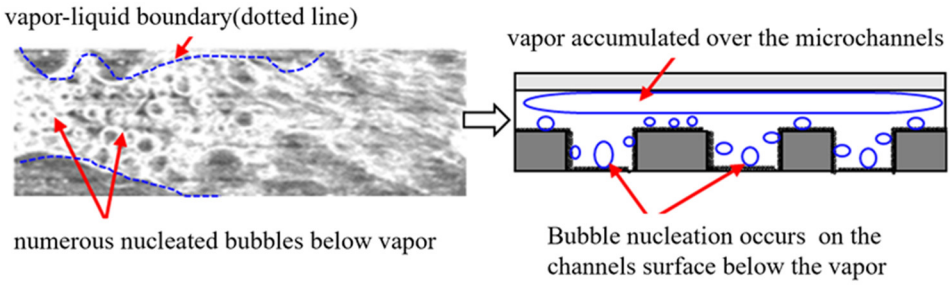

(**b**)

Figure 9. Typical flow patterns inside top-connected microchannels. **(a)**TCMC;**(b)** TCMC-Ni/Ag.

In the TCMC - Ni/Ag as depicted in Figure 9b, a substantial top-vapor and bottom-liquid film coverage area is observed in the top-connected region of the channel. On the surface of the Ni/Ag composite structure in the upstream of the channel, numerous nucleated bubbles of varying sizes are present. In this particular type of top-connected microchannel, within the top-connected region featuring a top - vapor and bottom - liquid film coverage configuration, the bubble nucleation phenomenon on the heating surface exhibits a notable congruence with the findings reported by Kalani and Kandlikar [12]. This correspondence implies that, under the specific conditions established by the co - presence of the top - vapor and bottom - liquid films in the top-connected area of the microchannel, the underlying mechanism governing bubble nucleation on the heating surface adheres to the patterns elucidated in the research of Kalani and Kandlikar [12]. Compared with the TCMC, the nucleated bubbles generated on the surface of the TCMC - Ni/Ag are smaller in size and greater in number. In the downstream of the TCMC - Ni/Ag channel, bubble nucleation is inhibited, and the flow pattern transitions to a regime dominated by thin - liquid - film convective evaporation.

The heat transfer enhancement mechanism of top-connected microchannels can be analyzed from the perspective of the channel geometric configuration and the resulting flow pattern distribution. For TCMC, on one hand, bubble nucleation occurs not only on the inner walls of the channels but also on the top surfaces of their rib walls. This leads to a higher density of nucleation sites compared to RMC, thus increasing the latent heat transfer between the gas - liquid two phases. On the other hand, the existence of the top-connected region in TCMC enables the gas - liquid interface to expand both along the flow direction and in the direction perpendicular to the flow during the bubble nucleation and expansion process in the microchannel. This can significantly suppress problems such as heat transfer instability and local liquid deficiency drying out in RMC channels. In RMC, due to wall constraints, bubbles can only expand rapidly along the flow direction, causing these issues. As a result, the heat transfer performance is improved. Research by Kalani and Kandlikar [12] also shows that in top-connected microchannels, bubbles nucleated on the heating surface can detach in a timely manner and gather in the top-connected region of the microchannel. The heating surface remains continuously wetted by the liquid and continues to generate bubble nucleation, thus significantly enhancing the heat transfer coefficient. Besides, the increase of heat transfer coefficients in RMC, TCMC, and TCMC - Ni/Ag with the increase in heating power is related to the number of activated nucleation sites on the heated surface. Under a certain degree of superheat, the size range of effectively activatable nucleation sites can be expressed as [17]:

$$\frac{r_{\min}}{r_{\max}} = \frac{\delta_t K_1}{2K_2}\left[1 \mp \sqrt{1 - \frac{8K_2\sigma T_{sat}}{\rho_v h_{fg}\delta_t \Delta T_w}}\right] \tag{6}$$

That is, as the heating power increases, the wall superheat increases, causing the size interval [r_{min} , r_{max}] of nucleation sites that can be activated to expand. This leads to an increase in the nucleation density on the heating surface, thereby achieving enhanced phase change heat transfer.

Based on the surface micro - structures of TCMC and TCMC - Ni/Ag shown in Figure 6, the surface of TCMC - Ni/Ag has a multi - scale pore structure. These multi - scale pores are fully activated

 doi:10.20944/preprints202502.1397.v1

with the increase of wall superheat, generating a large number of nucleated bubbles. Besides the nucleation density, the bubble nucleation frequency is also one of the important factors determining the heat transfer coefficient. Fritz et al. [18] provided the relationship between the bubble departure diameter and surface wettability:

$$D = 0.0208\theta\left[\frac{\sigma}{g(\rho_l - \rho_v)}\right]^{\frac{1}{2}} \quad (7)$$

where , σ , g , ρ_l , ρ_v represent the surface contact angle, the gas - liquid interfacial tension, the acceleration due to gravity, the liquid - phase density, and the vapor - phase density, respectively.

Jacob et al. [19] found that the relationship between the bubble departure diameter and frequency can be expressed as:

$$fD^n = \mathrm{C} \quad (8)$$

where f is the bubble departure frequency, D is the bubble departure diameter, n is an exponent related to the boiling process, and C is a constant. From equations (7) and (8), it can be seen that due to the relatively small surface contact angle of TCMC - Ni/Ag, the departure diameter of the bubbles generated on its surface is small, and the departure frequency is high, which is consistent with the visualization research results shown in Figure 9b.When the surface heat flux is high, the multiscale porous surface of TCMC - Ni/Ag has strong hydrophilicity, which facilitates the formation of an efficient heat transfer mode of thin liquid film convective evaporation [20]. That is, the hydrophilic multi - scale porous surface of TCMC - Ni/Ag has a large nucleation density and nucleation frequency under medium and low heat flux conditions, and forms a thin liquid film evaporation heat transfer mode under high heat flux conditions. This is the main mechanism for the significant increase in its heat transfer coefficient compared with RMC and TCMC.

5. Conclusions

Regular parallel microchannels (RMC), top-connected microchannels (TCMC), and top-connected microchannels featuring a Ni/Ag micro/nano composite surface structure (TCMC-Ni/Ag) were fabricated on a polished copper substrate via laser etching and brush-plating techniques. Utilizing anhydrous ethanol as the working fluid, a comparative investigation of flow boiling heat transfer within these three types of microchannels was conducted. The key findings are summarized as follows:

(1) Through the application of the brush - plating technique, the Ni/Ag composite microstructure was successfully prepared on the laser - etched copper surface. This process yielded a hydrophilic multiscale porous microstructure surface with a surface contact angle of 6.1°.

(2) The maximum local heat transfer coefficients of TCMC and TCMC - Ni/Ag attained 43.66 kW/m²·K and 179.84 kW/m²·K, respectively. These values represent an increase of 24.14% and 4.1-fold compared to the maximum local heat transfer coefficient of RMC. Moreover, the maximum average heat transfer coefficients of TCMC and TCMC - Ni/Ag reached 38.28 kW/m²·K and 116.98 kW/m²·K, respectively, signifying an elevation of 22% and 2.9 - fold relative to the average heat transfer coefficient of RMC.

(3) Visualization analysis indicated that subsequent to the detachment of bubbles formed on the TCMC - Ni/Ag surface, they accumulated in the top-connected region of the microchannel. Meanwhile, a substantial number of bubble nucleation continued to occur on the microchannel surface.

(4) The multiscale pore structure on the TCMC - Ni/Ag surface furnished an abundance of vaporization nuclei, thereby augmenting the bubble nucleation density. Additionally, the pronounced surface hydrophilicity not only enhanced the bubble nucleation frequency under medium heat flux conditions but also facilitated the formation of a thin - liquid - film convective

 doi:10.20944/preprints202502.1397.v1

evaporation heat transfer regime under high heat flux scenarios. This constitutes the primary mechanism underlying the significant enhancement of heat transfer.

In this research, the top-connected microchannel heat exchanger featuring a Ni/Ag composite micro/ nano structured surface was ingeniously designed and meticulously fabricated. This innovative design has led to a remarkable enhancement in the flow boiling heat transfer performance within the microchannels.

The significance of this achievement extends far-reaching. It not only represents a significant advancement in the fundamental understanding of heat transfer mechanisms at the micro - scale but also offers novel insights into the optimized design of high - efficiency phase change heat transfer surfaces. The unique Ni/Ag composite micro/ nano structure on the surface of the microchannel heat exchanger has demonstrated its efficacy in promoting bubble nucleation, enhancing liquid - vapor phase change, and ultimately improving the overall heat transfer efficiency.

Moreover, this study paves the way for the development of high-efficiency compact microchannel heat exchangers. The improved flow boiling heat transfer performance implies the potential for reducing the size and weight of heat exchangers while maintaining or even enhancing their heat transfer capabilities. This is of great importance in various applications, such as in the electronics industry where space is at a premium, and in the automotive and aerospace sectors where energy efficiency and compactness are crucial.

Looking ahead, this research could potentially inspire further investigations in multiple directions. For instance, in - depth exploration of the scalability of the fabrication process could be carried out to enable large-scale production of such high - performance heat exchangers. Additionally, studies on the long - term stability and durability of the Ni/Ag composite micro/nano structure under different operating conditions are needed. This would ensure the reliable operation of the heat exchangers in real-world applications. Moreover, the integration of this technology with other emerging heat transfer enhancement techniques could be explored to achieve even higher levels of heat transfer efficiency. Overall, this research serves as a springboard for future advancements in the field of heat transfer and thermal management.

Author Contributions: Methodology, Zeyu Xu; resources, Zeyu Xu and Xiangrui Zhai; investigation, Zeyu Xu, Wei Zhang, Qianqian Zhang, Xiangrui Zhai, Xufei Yang, Yajun Deng and Bo Yu; writing—original draft preparation, Zeyu Xu and Wei Zhang; writing—review and editing, Zeyu Xu and Wei Zhang; supervision, Wei Zhang and Bo Yu; project administration, Wei Zhang; funding acquisition, Wei Zhang, Yajun Deng and Bo Yu All authors have read and agreed to the published version of the manuscript.

Funding: The authors declare that this study received funding from the National Natural Science Foundation of China (52076015, U2141218, 52106073, 12405191), and the Beijing Natural Science Foundation (3232024). The funders were not involved in the study design, collection, analysis, interpretation of data, the writing of this article or the decision to submit it for publication.

Data Availability Statement: The original contributions presented in the study are included in the article, further inquiries can be directed to the corresponding author.

Conflicts of Interest: The authors declare no conflicts of interest.

Abbreviations

The following abbreviations are used in this manuscript:

RMC	Regular Microchannel
TCMC	Top connected Microchannel
TCMC-Ni/Ag	Top connected Microchannel with Ni/Ag composite surface structures

References

 doi:10.20944/preprints202502.1397.v1

1. Tuckerman, D. B.; Pease, R. F. W. High - Performance Heat Sinking for VLSI. *IEEE Electron Device Lett.*, **1981**, 2(3), 129 - 169.
2. Li, Y.F.; Zhu C.T.; Li, C.M.; Yang, B. A Review of Non-Uniform Load Distribution and Solutions in Data Centers: Micro-Scale Liquid Cooling and Large-Scale Air Cooling. *Energies*, **2025**, 18(1), 149.
3. Jiang, H. Y.; Zhao, X. C.; Zhang, M. Boiling Heat Transfer Characteristics of Noah-2100A and HFE-649 in Pin-Fin Microchannel Heat Sink. *Energies*, **2024**, 17(24), 6216.
4. Yih, J.; Wang, H. L. Experimental characterization of thermal - hydraulic performance of a microchannel heat exchanger for waste heat recovery. *Energy Convers. Manag.*, **2020**, 204, 112309.
5. Asadi, M.; Xie, G. N.; Sunden, B. A review of heat transfer and pressure drop characteristics of single and two - phase microchannels. *Int. J. Heat Mass Transf.*, **2014**, 79, 34 - 53.
6. Patil, M. S.; Seo, J. H.; Panchal, S. Investigation on thermal performance of water - cooled Li - ion pouch cell and pack at high discharge rate with U - turn type microchannel cold plate. *Int. J. Heat Mass Transf.*, **2020**, 155, 119728.
7. Tan, H.; Wu, L. W.; Wang, M. Y.; Yang, Z. H.; Du, P. A. Heat transfer improvement in microchannel heat sink by topology design and optimization for high heat flux chip cooling. *Int. J. Heat Mass Transf.*, **2019**, 129, 681 - 689.
8. Zong, L. X.; Xia, G. D.; Jia, Y. T.; Liu, L.; Ma, D. D.; Wang, J. Flow boiling instability characteristics in microchannels with porous - wall. *Int. J. Heat Mass Transf.*, **2020**, 146, 118863.
9. Serrao, B.P.; Kim, K.M.; Duarte, J.P. Analysis of the Effects of Different Nanofluids on Critical Heat Flux Using Artificial Intelligence. *Energies*, **2023**, 16(12), 4762.
10. Qu, W. L.; Mudawar, I. Measurement and correlation of critical heat flux in two - phase micro - channel heat sinks. *Int. J. Heat Mass Transf.*, **2004**, 47(10 - 11), 2045 - 2059.
11. Tibirica, C. B.; Czwlusniak, L. E.; Ribatski, G. Critical heat flux in a 0.38mm microchannel and actions for suppression of flow boiling instabilities. *Exp. Therm. Fluid Sci.*, **2015**, 67, 48 - 56.
12. Kalani, A.; Kandlikar, S. G. Flow patterns and heat transfer mechanisms during flow boiling over open microchannels in tapered manifold (OMM). *Int. J. Heat Mass Transf.*, **2015**, 89, 494 - 504.
13. Yin, L. F.; Jiang, P. X.; Xu, R. N., Hu,X.W.; Jia, L. Heat transfer and pressure drop characteristics of water flow boiling in open microchannels. *Int. J. Heat Mass Transf.*, **2019**, 137, 204 - 215.
14. Yin, L. F.; Jiang, P. X.; Xu, R. N., Wang, W.T.; Jia, L. Visualization of flow patterns and bubble behavior during flow boiling in open microchannels. *Int. Commun. Heat Mass Transf.*, **2017**, 85, 131 - 138.
15. Zhao, Y. D.; Zhang, W.; Wu, Z. Y.; Sun, Y.Z.; Xu, J.L. Experimental study on flow boiling heat transfer in open parallel microchannels. *J. Eng. Thermophys.*, **2018**, 39(7), 1498 - 1504.
16. Chen, X. L.; Nan, J. M.; Zhang, Y. Preparation and tribological performance of Ni - SiC composite coating on 304 stainless steel through brush plating. *Surf. Coat. Technol.*, **2024**, 49, 131491.
17. Hsu, Y. Y. On the size range of active nucleation cavities on a heating surface. *J. Heat Transf. - Trans. ASME*, **1962**, 84, 207–213.
18. Fritz, W. Maximum volume of vapor bubbles. *Physik Zsitsehr.*, **1935**, 36, 379.
19. Jacob, M. *Heat Transfer*[M]. Wiley, **1949**, New York.
20. Zhang, W.; Chai, Y. Z.; Xu, J. L. 3D heterogeneous wetting microchannel surfaces for boiling heat transfer enhancement. *Appl. Surf. Sci.*, **2018**, 457, 891 - 901.